Total internal reflection Raman spectroscopy

Phillip R. Greene and Colin D. Bain
Department of Chemistry, University of Oxford, Chemistry Research Laboratory, Mansfield Road, Oxford, OX1 3TA, UK.
E-mail: colin.bain@chem.ox.ac.uk

Introduction

Within the last two decades, Raman spectroscopy has become established as a fast, non-invasive, non-destructive analytical tool. Development of commercial Raman spectrometers has been spurred on by technological improvements in lasers, optical filters and charge-coupled device (CCD) detectors. Modern Raman microspectrometers achieve high sensitivity from liquids and solids with volumes of only a few femtolitres. However, the sensitivity and spatial resolution of commercial Raman systems is not yet sufficiently good to allow routine characterisation of ultrathin (<5 nm thickness) films at interfaces without the use of enhancement mechanisms, such as electronic resonances or surface plasmons in roughened metal surfaces achieved with surface-enhanced Raman scattering (SERS).

Raman scattering by evanescent waves was first demonstrated by Ikeshoji *et al.* in 1973.[1] Although this early work used a bulk sample, it demonstrated the potential for obtaining unenhanced Raman spectra of ultrathin films at interfaces. Largely due to the explosive growth of SERS in the 1970s, the alternative approach of total internal reflection (TIR)-Raman spectroscopy received little attention. With modern commercial instrumentation, however, TIR-Raman can be applied to a wide range of different physical and chemical systems, without some of the restrictions imposed by surface or resonance enhancement. This article provides an introduction to the principles and practice of TIR-Raman spectroscopy, and outlines recent developments of the technique. We focus on examples from our own research group, where we have used TIR-Raman spectroscopy to study films from nanometres to micrometres in thickness. In all cases, our experiments were carried out on a modified commercial Raman spectrometer (Renishaw System 1000) equipped with a 2 W frequency-doubled Nd:YVO_4 laser operating at 532 nm (Millenia 2, Spectra-Physics).

Total internal reflection

There are two basic requirements for TIR-Raman scattering from a thin film at an interface. The first is that the interface is accessible to light from at least one side. The second is that the medium through which the laser beam is delivered has a higher refractive index than the second medium. Under these conditions, it is possible to arrange that the laser beam is totally reflected at the interface with only an evanescent wave penetrating into the second medium. It is this evanescent wave that generates the Raman spectrum from the thin film at the interface. Figure 1 shows two sample geometries that we have employed: scattered light can be collected either through the prism [Figure 1(a)] or through the sample itself [Figure 1(b)], if the sample is transparent.

The principles of total internal reflection will be familiar to readers experienced with attenuated total reflection Fourier transform infrared (ATR-FTIR) spectroscopy. We will summarise here the salient features of the theory of TIR and use them to illustrate how a TIR geometry can confer surface-selectivity and improved sensitivity on Raman spectroscopy.

Surface selectivity

A beam of light incident on an interface is bent away from the surface normal as it passes from the optically more-dense medium (i.e. that having higher refractive index) to the optically less-dense medium. The reflected portion of the beam is said to undergo internal reflection. There exists a critical angle of incidence, θ_c, above which all of the light is reflected back into the optically dense medium and none of the incident energy is transmitted into the optically rarer

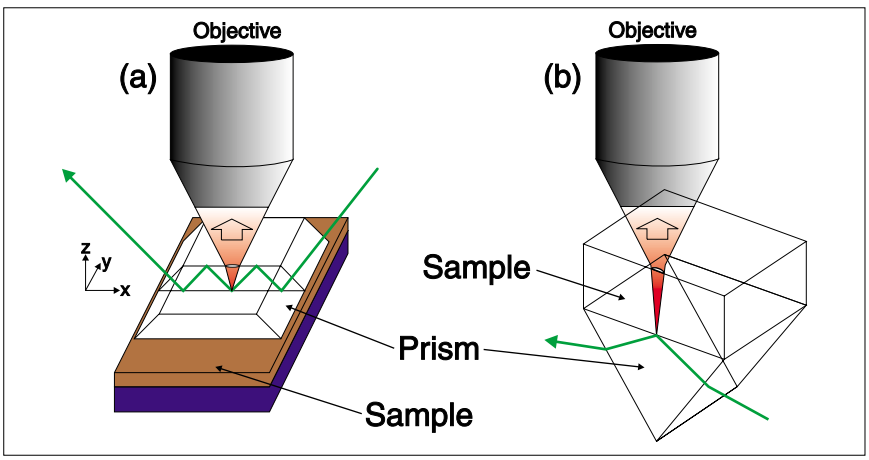

Figure 1. Schematic diagrams showing configurations for TIR-Raman spectroscopy of an opaque (a) or a transparent (b) sample. For clarity, schematic (a) shows a cross-section through the incident plane.

medium, i.e. there is total internal reflection. From Snell's Law, $\theta_c = \sin^{-1} n_{ti}$, where $n_{ti} = n_t / n_i$ and n_t and n_i are the refractive indices of the transmitting and incident medium, respectively. Although there is no flux of energy across the interface, there is still an electromagnetic field in the second medium in order to satisfy the boundary conditions on the electric and magnetic fields at the interface.[2] The transmitted wave propagates along the surface in the plane of incidence with its electric field, E, decaying exponentially with distance, z, normal to the interface [Equation (1)]. For this reason, it is known as an evanescent ("quickly fading") wave.

$$\frac{E}{E_0} = \exp(-\beta z)$$

$$\text{where } \beta = \frac{2\pi}{\lambda}\left(\frac{\sin^2\theta_i}{n_{ti}^2} - 1\right)^{1/2} \qquad (1)$$

β is the electric field amplitude decay coefficient, θ_i is the angle of incidence, λ is the wavelength of incident light and E_0 is the electric field at $z = 0$. The penetration depth, d_p, of the electric field, into the optically rarer medium is given by $d_p = 1/\beta$. Except for angles very close to θ_c, d_p is less than λ, and the electric field becomes negligible at a distance of only a few wavelengths into the second medium. Since incoherent Raman scattering is proportional to the intensity of the incident light, and hence E^2, the Raman signal, drops off twice as fast as the electric field: >98% of the Raman signal originates from a distance $<2d_p$ from the interface. Figure 2 illustrates how the penetration depth of the squared electric field depends on the angle of incidence. Note that $d_p \rightarrow \infty$ as $\theta_i \rightarrow \theta_c$.

As in ATR-IR, the penetration depth is minimised when the relative refractive index n_{ti} is smallest (i.e. when incident media have high refractive indices). Materials such as cubic zirconia (ZrO_2), with a refractive index of 2.2, low fluorescence and no substrate bands at wavelengths >700 cm^{-1} make for good coupling prisms in TIR-Raman spectroscopy.

Since d_p varies with λ, TIR-Raman spectroscopy has some advantages over ATR-IR spectroscopy in that TIR-Raman experiments employ monochromatic laser beams with a shorter wavelength. Thus the penetration depth for a TIR-Raman spectrum is small and constant at all wavenumbers in a given spectrum. Since d_p varies with θ_i, it is possible, in principle, to obtain a depth profile of the surface of a sample simply by changing the incident angle. As Figure 2 shows, tight control over the incident angle is required for depth profiling by this method.

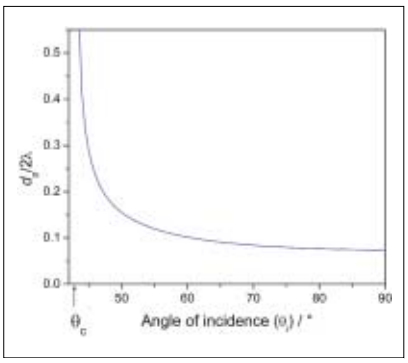

Figure 2. Variation of penetration depth of the squared electric field $d_p / 2$, relative to the wavelength, λ, of the laser, as a function of the angle of incidence (θ_i), for TIR at the interface between a cubic-zirconia prism ($n = 2.2$) and a polymer ($n = 1.5$).

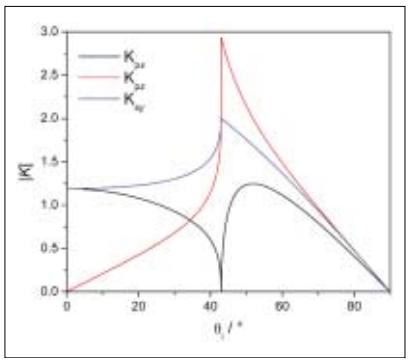

Figure 3. Graph showing the variation of Fresnel factors (| K |) with angle of incidence, for beams of different polarisation, incident through a cubic-ZrO_2 phase ($n = 2.2$) onto an interface with a polymer of refractive index 1.5. The first subscript of K gives the polarisation of the incident electric field, while the second subscript describes the field at the interface.

Improved sensitivity

The relative proportion of incident energy transmitted and reflected from an interface depends on the incident angle, the ratio of refractive indices across the interface, and the polarisation of the incident light. The electric field in a thin film at an interface is related to the field in the incident medium by Fresnel factors,[2] which we will label K. For example, the K-factor for a conventional confocal Raman spectrometer in which the laser beam is at normal incidence in air onto a polymer with a refractive index of 1.5 would be 0.8.

In Figure 3, we have plotted Fresnel factors for the interface between a ZrO_2 prism and the same polymer. The subscripts of each K-factor refer to the polarisations of the incident beam (s- or p-polarised) and the polarisation of the field at the interface (x, y or z; the plane of incidence is the xz plane, with z as the surface normal). Light polarised parallel to the incident plane (p-polarised) is independent of light polarised perpendicular to the incident plane (s-polarised) in isotropic media. p-Polarised incident light will, in general, give rise to fields in the x and z directions and s-polarised light to a field in the y direction.

The dependence of the K-factors on incident angle (Figure 3) has two important aspects. First, K_{pz} and K_{sy} are maximised when light is incident at the critical angle. The K-factors at θ_c are several times greater than for normal incidence. Even after allowing for transmission through the air–prism interface, E_y^2 (which determines the strength of an s-polarised Raman spectrum) in the TIR geometry is 1.6 times greater than in normal incidence through air.

The second feature is that K_{px} becomes zero at the critical angle. Consequently, a p-polarised beam incident at θ_c produces an interfacial electric field that oscillates purely in the z-direction. The special case of TIR at θ_c is the only way to produce an electric field with purely z-oscillations at a dielectric interface. TIR therefore enables more components of the Raman polarisability tensor to be measured than does conventional beam delivery along the surface normal.

Practical considerations

There is no surface sensitivity exactly at the critical angle, but with an incident angle slightly larger than θ_c, we can achieve a good compromise between

Corner the Performance Advantage with JASCO FT-IR

Introducing the New FT/IR-4000 and FT/IR-6000 Series

Highly Stable Corner Cube Interferometer with AccuTrac™ DSP Technology Guarantees the Highest Level of Performance.

- Robust High Sensitivity FT-IR Systems for a Wide Range of Routine and Critical Analysis Application
- IQ Accessory Recognition System Programmable for any Commercially Available Sampler
- Rapid Scan and Step Scan Options for Real Time Analysis of Reaction Kinetics and Time Resolved Imaging

With over forty years of experience in infrared spectroscopy, JASCO introduces a new series of advanced FT-IR instrumentation and sampling accessories.
The FT/IR-4000 and FT/IR-6000 Series set a whole new standard for performance, flexibility, and ease of operation. Each compact model offers unsurpassed reliability and the highest signal-to-noise ratio in the industry.
Whatever your application or budget there's a perfect JASCO FT-IR solution...not only for today but for tomorrow.

JASCO Comparison Proven

FASTLINK / CIRCLE 006 FOR FURTHER INFORMATION

JASCO EUROPE s.r.l.
Via Confalonieri 25, 22060 Cremella (Co), Italy Tel: +39-039-956439 Fax: +39-039-958642 Internet: http://www.jasco-europe.com
JASCO INTERNATIONAL CO., LTD., 4-21, Sennin-cho 2-chome, Hachioji, Tokyo193-0835, Japan Tel: +81-426-66-1322 Fax: +81-426-65-6512 Internet: http://www.jascoint.co.jp/english/index.html
JASCO INCORPORATED, 8649 Commerce Drive, Easton, Maryland 21601-9903, U.S.ATel:+1-800-333-5272 Tel:+1-410-822-1220 Fax:+1-410-822-7526 Internet:http://www.jascoinc.com

FT-IR ● UV-Vis ● Fluorescence ● Chiroptical ● Chromatography

depth sensitivity (Figure 2) and interfacial electric field (Figure 3). Typically the evanescent wave penetrates to a depth of <200 nm, imparting excellent depth resolution compared to confocal Raman spectroscopy, which usually achieves a depth resolution of ~2 µm at best.

In cases where depth resolution is not important, operating at the critical angle gives optimum sensitivity. Several other factors can improve the sensitivity of TIR-Raman techniques compared to confocal Raman experiments. Where the required depth discrimination is provided by TIR, the microscope can be used simply as efficient collection optics (not as a means to reduce the depth of focus). Consequently, the field of view of the detection optics can be increased without compromising the depth resolution. A large area of the interface then contributes to the signal and produces spectra with higher signal-to-noise ratios. Since larger laser spots can be employed, higher laser powers can be used without exceeding the damage threshold of the sample. Delivering the laser beam independently of the collection optics also allows the use of higher laser powers. Only scattered light enters the microscope and the scattering intensity is too low to damage the objectives and beam splitters. In combination, these factors can result in a signal-to-background improvement of two orders of magnitude in TIR-Raman scattering compared to confocal Raman spectroscopy.[3]

Applications

Polymer laminates

Polymer films a few hundred micrometres thick are commercially important in applications such as plastic bags and soft-drink bottles. Polymers are often laminated with thin coatings of other polymers to modify the surface properties and much effort is directed towards the characterisation of these surface films. Figure 4 shows a TIR-Raman spectrum from a 2.5 µm coating of PEN [poly(ethylene naphthalate)] on PET [poly(ethylene terephthalate)] acquired by pressing the polymer against a cubic-ZrO_2 prism [Figure 1(B)]. The red spectrum was obtained with $\theta_i < \theta_c$, in which case the bulk polymer film is sampled and both the PEN and PET peaks are clear. The blue spectrum was obtained with $\theta_i > \theta_c$ (TIR) and only the PEN peaks are observed. In a confocal Raman spectrum of the same laminate (not shown), the peak at 1615 cm^{-1} from the PET substrate was still visible.

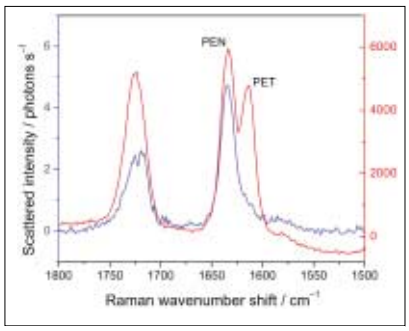

Figure 4. Raman spectra of PEN (2.5 µm thick) on the surface of a PET film (200 µm thick): (red) $\theta_i < \theta_c$; (blue) $\theta_i > \theta_c$ (TIR). Conditions: 532 nm, 0.2 W, 10 s red) 5 min (blue), Olympus ULWD 50× dry objective.

Frictional contacts

Friction in solid–solid contacts can be reduced by ultrathin films of boundary lubricants, which are often no thicker than a monolayer. TIR-Raman spectroscopy can provide molecular-level detail about monolayers at solid–solid interfaces, if we arrange that at least one of the solids is an optical component.

Figure 5(a) shows a spectrum of a Langmuir–Blodgett (LB) monolayer of zinc arachidate [$Zn(C_{19}H_{39}CO_2)_2$] at the interface between a CaF_2 prism and an MgF_2 lens. The sensitivity of unenhanced TIR-Raman scattering is sufficient to provide monolayer spectra of excellent quality in only a few minutes. The use of one curved and one planar surface imparted a well-defined contact area with an average pressure of 90 MPa, and the lateral resolution of our experiments (~30 µm) is sufficient to examine only the centre of the region of contact between the two surfaces. Comparison with a TIR-Raman spectrum from the CaF_2–air interface shows that the application of pressure does not cause major disruption of the monolayer [Figure 5(a)]. Since the monolayer peaks fall in regions of the spectrum where the substrates give no signal, exclusion of bulk signals was

ELAN eliminates the element of surprise from ICP-MS.

High throughput, yes. High sensitivity, yes. High blood pressure, no way. With an ELAN® 9000, DRC-e or DRC II, the excitement of ICP-MS is in performance and results. You won't get any training or downtime surprises because we promise (and deliver!) turnkey methods to get you up and running quickly. Plus, all ELAN systems provide maximum uptime with minimal maintenance.

We've been the inorganic analysis leader ever since AA, so it's no wonder we're the name you can trust for ICP-MS. If you'd like to experience astonishing productivity at the detection levels you need, talk to a PerkinElmer ICP-MS specialist and be sure to ask for a free *Guide to ICP-MS.* You can also request a guide, or sign up for one of our Web seminars, at www.perkinelmer.com/ICPMS.

CIRCLE 008 FOR SALES CIRCLE 009 FOR LITERATURE

PerkinElmerSCIEX™

800-762-4000 (U.S. and Canada)
(+1) 203-925-4602

www.perkinelmer.com

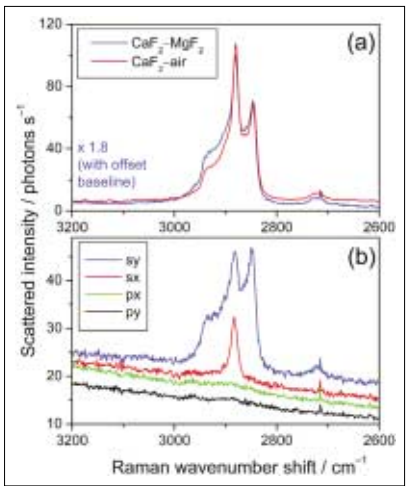

Figure 5. (a) A TIR-Raman spectrum of an LB monolayer of zinc arachidate on a CaF_2 prism in air, overlaid with a spectrum of the film confined between a CaF_2 prism and an MgF_2 lens under ~90 MPa pressure; (b) polarisation-resolved TIR-Raman spectra of an LB monolayer of zinc arachidate on a silica prism in contact with an LB monolayer of deuterated zinc arachidate on a CaF_2 lens. Conditions: (a) 0.9 W, 532 nm, s-polarised, 15 min, $\theta_i = 49°$ (solid–air interface) or $\theta_i = 78°$ (solid–solid interface), Olympus ULWD 50× dry objective; (b) similar, except $\theta_i = 80°$, ~33 MPa pressure, 5 min (s-polarised) or 10 min (p-polarised).

not a major concern in this system. To maximise sensitivity, the angle of incidence was very close to the critical angle, and scattered light was collected from a relatively large area at the interface (~500 μm^2).

Spectra recorded from the solid–solid contact under different polarisation conditions (sx, sy, px, py) are shown in Figure 5(b). The absence of peaks in the px and py spectra demonstrate that the hydrocarbon chains in the monolayer are oriented perpendicular to the interface.

Silica–water interface

For our third example, we consider TIR-Raman spectroscopy of lipids and surfactants adsorbed at the silica–water interface. These systems demand sensitivity to one or two monolayers of surfactant as well as suppression of the bulk signals from dissolved surfactants and water. Spectra from a single bilayer of egg lecithin adsorbed at the silica–water interface are shown in Figure 6. The small penetration depth (~220 nm) of the evanescent wave restricts the size of the water peaks, facilitating subtraction to yield clear spectra of an immersed phospholipid bilayer, even in the fingerprint region. The stretching mode of the carbon–carbon double bond (at 1650 cm^{-1}) is readily detected, even though there is only one such bond for every two lipid chains. The relative intensities of peaks in spectra with different polarisations could be used to infer the orientation of particular functional groups in such artificial membranes.

Experiments with bilayers of soluble surfactants adsorbed on silica have shown that, for a concentration of 1 mM, surfactant molecules dissolved in the bulk solution within the evanescent wave typically contribute only ~4% of the total surfactant signal in TIR-Raman spectra. At higher concentrations the relative importance of the bulk surfactant signal increases, but it is relatively straightforward to account for the bulk contributions to spectra.

Leaves

The outermost layer of a leaf surface is called the cuticle. The most important fraction of foliar cuticles comprises cuticular waxes – a multiphase system that is typically between 100 nm and 1 µm thick and contains crystalline, solid amorphous and liquid amorphous components. Foliar wax layers have mostly been studied in the past as extracted, reconstituted wax, and by techniques such as chromatography which are necessarily invasive, destructive and *in vitro*. Little is known about the structures and properties of cuticular wax layers *in vivo*.

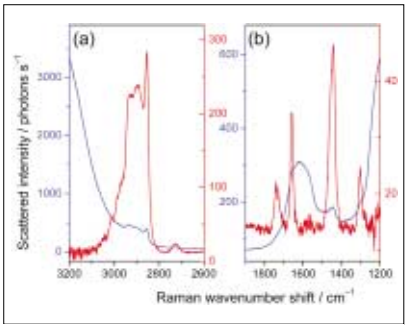

Figure 6. TIR-Raman spectra of a bilayer of egg lecithin (palmitoyl oleoyl phosphatidylcholine, POPC) at the silica–water interface, before (blue) and after (red) subtraction of the pure buffer spectrum. Note that residual noise levels after subtraction are larger in regions with large background signals. Conditions: 532 nm, 1.8 W, incident beam s-polarised, collected light polarised in y-direction, $\theta_i = 68°$, Zeiss 40× water immersion objective, 350 s [CH stretching region, (a); 1200 s (fingerprint region, (b)].

With TIR-Raman scattering, it has been possible to obtain spectra from the cuticular waxes on the surface of living barley leaves (see Figure 7). The ratio of peak intensities for the antisymmetric (2882 cm^{-1}) and symmetric methylene modes (2851 cm^{-1}) indicates that the surface waxes are crystalline. Our TIR-Raman studies of leaves also contributed evidence for trace amounts of carotenoids in the cuticular waxes.

Spectra of cuticular waxes provide a particularly elegant demonstration of TIR-Raman spectroscopy, since leaves present a number of practical obstacles. Leaf surfaces are rough and may be easily damaged by pressure; contact with a prism is imperfect, but the technique still has ample sensitivity. Notably, our spectra were recorded with a 532 nm (green) laser, yet the spectra contain minimal fluorescence from the underlying leaf constituents and pigments. It is possible to avoid fluorescence from plant material

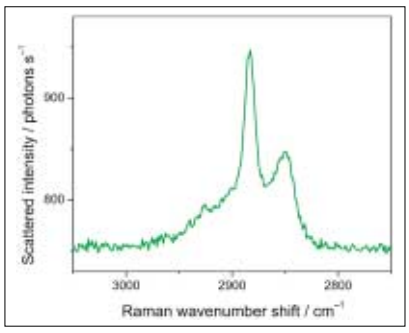

Figure 7. TIR-Raman spectrum of cuticular waxes on the surface of a barley leaf, pressed against a cubic-ZrO_2 prism. The prism adds two broad humps to the baseline (at 3040 cm^{-1} and 2700 cm^{-1}), which have been removed by subtraction. Conditions: 0.2 W, 10 min, 532 nm, s-polarised, laser spot size ~(20 × 30) mm, $\theta_i = 56°$, Olympus ULWD 50× dry objective.

with infrared probe beams, but not without significantly reducing the sensitivity and depth resolution. We employed a high incident angle that limited the penetration depth d_p / 2 to 60 nm (refer to Figure 2), so the laser field was confined to the wax layers. Leaves are susceptible to laser damage as well, but the barley was not burned because it was only exposed to the evanescent wave, the laser spot was relatively large (therefore low in intensity), and the prism acted as an efficient heat sink.

Conclusions

Both in theory and in practice, TIR-Raman spectroscopy offers several advantages over conventional Raman scattering methods. The main benefits associated with TIR-Raman techniques are excellent depth resolution and improvements in the strength of the incident field due to favourable electric field effects. Since depth resolution arises from the evanescent wave and not from the confocal parameter of a tightly focussed laser beam, it is possible to use relatively large laser spots (>10 µm diameter), higher laser powers and wide entrance apertures on the spectrometer, leading to higher-quality spectra, shorter acquisition times and less sample damage.

We have shown that TIR-Raman scattering can be used to study an assortment of interfaces, simple and complex, robust and delicate. All the TIR-Raman experiments were based on a commercial Raman microscope and a conventional laser system. While commercial accessories for TIR-Raman are not yet available, there is no reason why TIR-Raman scattering should not take its place as a standard technique in the toolbox of the vibrational spectroscopist, just as diamond ATR systems have done for infrared absorption spectroscopy.

Acknowledgements

We would like to thank the following members of the Bain research group, who supplied some of the data presented in this article: Chongsoo Lee (egg lecithin spectra), Sarah Haydock and David Beattie (zinc arachidate spectra). Laminated polymer samples were kindly provided by Neil Everall (ICI plc). The work was supported by Syngenta and the EPSRC.

References

1. T. Ikeshoji, Y. Ono and T. Mizuno, *Appl. Optics* **12,** 2236 (1973).
2. M. Born, E. Wolf and A.B. Bhatia, *Principles of optics: electromagnetic theory of propagation, interference and diffraction of light*. Cambridge University Press (1999).
3. D.A. Beattie, S. Haydock and C.D. Bain, *Vib. Spectrosc.* **24,** 109 (2000).